SAE Technical Paper Series

810149

Fast Sampling Valve Measurements of Hydrocarbons in the Cylinder of a CFR Engine

P. Weiss
and J. C. Keck
Massachusetts Institute of Technology

International Congress and Exposition
Cobo Hall, Detroit, Michigan
February 23-27, 1981

SOCIETY OF AUTOMOTIVE ENGINEERS, INC.
400 COMMONWEALTH DRIVE
WARRENDALE, PENNSYLVANIA 15096

810149

Fast Sampling Valve Measurements of Hydrocarbons in the Cylinder of a CFR Engine

P. Weiss
and J. C. Keck
Massachusetts Institute of Technology

ABSTRACT

A time resolved study of the unburned hydrocarbons in the cylinder of a spark ignition engine has been made. A fast acting needle value was used to sample the gas near the cylinder wall opposite the spark plug. The volume sampled was measured by water displacement and the total hydrocarbon mole fraction was measured with a flame ionization detector. Measurements were made as a function of crank angle over the entire engine cycle for a range of equivalence ratios, inlet pressures, spark advances, inlet temperatures, and EGR fractions. Average hydrocarbon concentrations in the exhaust were also measured. Two possible sources of post combustion hydrocarbon in the cylinder were considered: thin wall quench layers and fine crevices into which a flame cannot propagate. The results suggest that crevices were the source of the hydrocarbon. Models for predicting hydrocarbon from both quench layers and crevices were developed and are presented.

THE DISPOSAL OF INDUSTRIAL AND TRANSPORTATION VEHICLE WASTE poses a serious threat to the environment. Increasing concern for improved air quality has directed our attention towards understanding the mechanisms of formation and behavior of the toxic components of the exhaust from spark ignited engines. One such component is unburned hydrocarbon. It was first suggested by W. A. Daniel [1 - 3] that flame quenching on the relatively cool combustion chamber walls is a source of exhaust hydrocarbon. Other sources which have been suggested are crevice volumes into which a flame cannot propagate [4,5], oil layers [6], and bulk quenching [7].

Many measurements of flame quenching distances at cool surfaces have been made [8 - 11] and models for correlating the results have been developed [12 - 15]. Exhaust hydrocarbons from combustion bombs [16] and engines [17,18] have also been measured and analysis of the data has tended to support the conclusion that quench layers were a major source of exhaust hydrocarbon from engines [19]. Although this conclusion has been generally accepted for many years, recent theoretical calculations [20,21] have predicted virtually complete oxidation of the quench layer hydrocarbons as a result of diffusion into the hot combustion products. This prediction has since received strong support from in-cylinder sampling experiments [22] and from measurements of exhaust hydrocarbons from bombs having very small crevice volumes [23 - 25].

To procure further information regarding the source of exhaust hydrocarbons from engines, a parametric study of both exhaust and in-cylinder hydrocarbons has been carried out in a CFR engine operating at 1000 RPM on isooctane. Samples of the gas near the cylinder wall of the engine were taken over a complete engine cycle using a rapid

0148-7191/81/0223-0149$02.50

acting sample valve. These samples as well as samples from the exhaust were analyzed for total hydrocarbon using a flame ionization detector. The procedure and results are presented in the following sections.

EXPERIMENTAL FACILITY

CFR TEST ENGINE - A schematic diagram of the test engine and associated equipment is shown in Fig. 1. Table 1 gives the relevant CFR specifications. The engine used in this investigation was coupled to a D.C. dynamometer to provide free motoring and firing capabilities. The fueling system used a heated mixing tank to supply a fully vaporized fuel-air charge. A high pressure burner nozzle atomized the fuel entering the mixing tank. Fuel flow rates were measured and regulated using a rotometer. The nitrogen propelled fuel was cooled upstream of the rotometer to prevent cavitation and thus facilitate accurate metering. Air was delivered to the mixing tank from a large surge tank. Engine load was controlled with a throttle valve and air flow rates were measured using a sharp edged orifice. The exhaust system consisted of an exhaust pipe which fed a surge tank which in turn was connected to the laboratory exhaust trench. The exhaust surge tank was equipped with a tap for withdrawing gas for emissions analysis. Exhaust gas recirculation, EGR, was accomplished by a heated pipe connecting the exhaust pipe with the mixing tank. EGR flow rates were regulated by a throttle value and metered with a sharp edged orifice. External pumps and heat exchangers were employed by the lubricating and cooling systems. A breakerless solid state ignition system was used.

Table 1 - CFR Specifications

Parameter	Value
Bore	8.3 cm
Stroke	11.4 cm
Connecting Rod Length	25.4 cm
Clearance Volume @ C.R. = 7.3:1	98 cm^3
Clearance Height @ C.R. = 7.3:1	1.6 cm
Radius from Cylinder Centerline to Spark Plug	4.1 cm
Intake Valve - opens	10 deg. a.t.d.c.
- closes	34 deg. a.b.d.c.
Exhaust Valve - opens	40 deg. b.b.d.c.
- closes	15 deg. a.t.d.c.
Valve Lift	0.79 cm
Piston Crevice Volume	0.74 cm^3
Displacement Volume	617 cm^3

SAMPLING SYSTEM - Fig. 2 shows a drawing of the sample valve. The valve was of the magnetically driven inward opening needle type. Needle lift and sample duration were monitored using a proximity probe. Needle lift was regulated by adjusting the gap between the valve coil and needle assembly. The original General Motors Research Laboratory design employed a stainless steel needle and titanium alloy seat. This combination resulted in an unacceptable leak rate for sampling in-cylinder hydrocarbon. At low engine speeds, a ccpper seat reduced the sample valve leak rate to acceptable levels.

A schematic of the sampling system is shown in Fig. 3. The sample valve was located

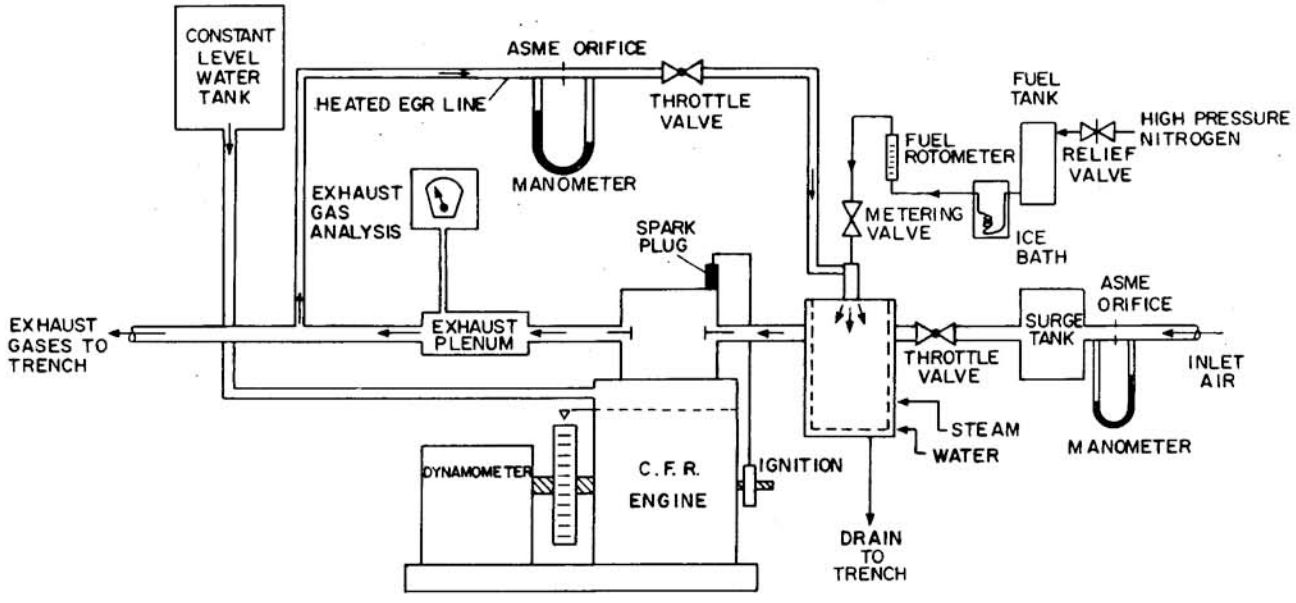

Fig. 1 - Schematic diagram of CFR engine and associated equipment

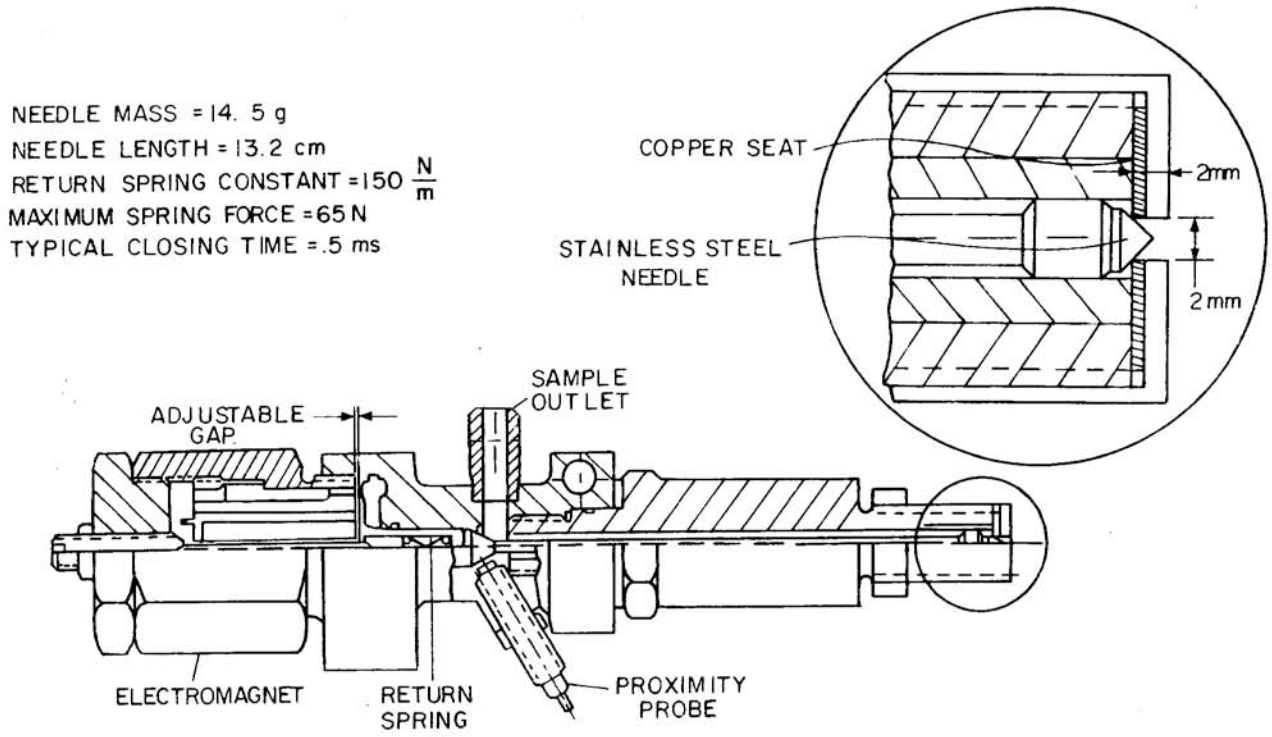

Fig. 2 - Modified GMR sampling valve

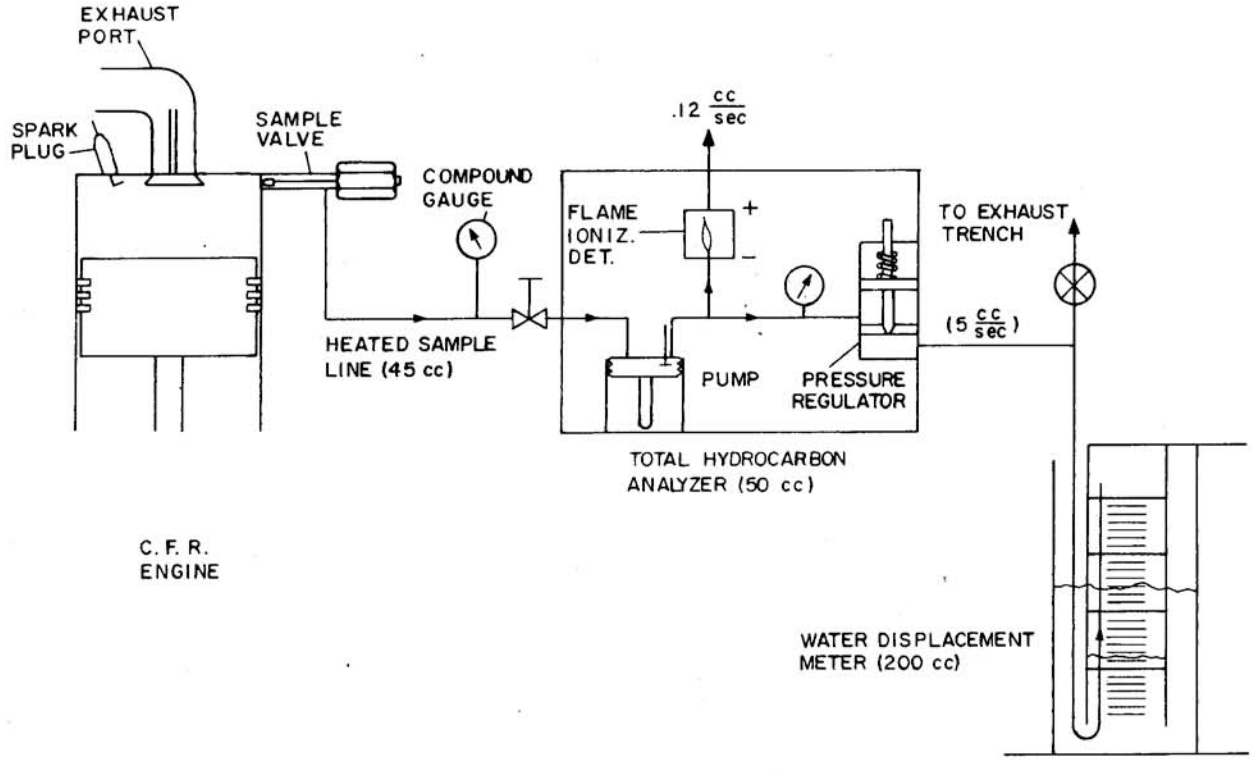

Fig. 3 - Schematic diagram of continuous flow gas sampling system

in the clearance volume flush with the cylinder wall and opposite the spark plug. Sampled gas was delivered to a heated total hydrocarbon analyzer through a heated stainless steel line. A water displacement meter was used to measure sample flow rates. A throttle valve was located on the upstream side of the hydrocarbon analyzer.

ELECTRONIC AND CONTROL SYSTEM - Fig. 4 shows a block diagram of the electronic and control systems. A piezoelectric pressure transducer was used to monitor instantaneous cylinder pressure. The cylinder pressure signal was displayed on an oscilloscope and was also digitized and filed with the aid of a computer and analog to digital converter. A rotary generator supplied a voltage pulse for each degree of rotation. Every tenth pulse was displayed on the oscilloscope to provide 10° crank angle markers. The output of the rotary generator was also processed to provide an oscilloscope sweep trigger and a digital engine speed display. Sample valve phasing was accomplished using the delayed trigger from the oscilloscope. The sample valve controller was capable of adjusting sample phasing and duration.

EXPERIMENTAL PROCEDURE AND RESULTS

Sampling System Operation - The sampling system was brought on line by turning on the hydrocarbon analyzer pump and heating the sample line and hydrocarbon analyzer flame ionization detector to their stable operating temperature of approximately 450° K. Sample valve parameters (i.e., needle lift, sample duration, and return spring force) were also adjusted at this time. Sampling was then initiated at peak pressure in a motored engine. The sample flow was throttled in order to pressurize the sample line and liquid leak detector was used to check for leaks at the sample fittings. Next, the sample valve was switched off and the sample valve leak rate was measured by completely closing the sample line throttle valve and timing the change in pressure of the sample line.

When satisfactory system performance was achieved for motoring conditions, sampling in a firing engine was the next step. After stable engine operation was achieved, the hydrocarbon analyzer was calibrated and the sample valve was switched on. Sample valve parameters were readjusted to compensate for the needle assembly elongation that resulted from sampling hot combustion gases. After an initial leak rate measurement had been completed, sampling began. The sample flow rate was measured by timing the water elevation change in the displacement meter. Sample hydrocarbon mole fractions were measured by selecting the appropriate scale on the hydrocarbon analyzer electrometer and directly reading the indicated value. After the sample measurements were completed, the leak rate was measured again. The sample phasing was then readjusted and the sampling process was repeated. Initially, leak rates were measured before and after each sampling run. If the leak rate remained relatively constant for a long period of time, leak measurements were made less frequently.

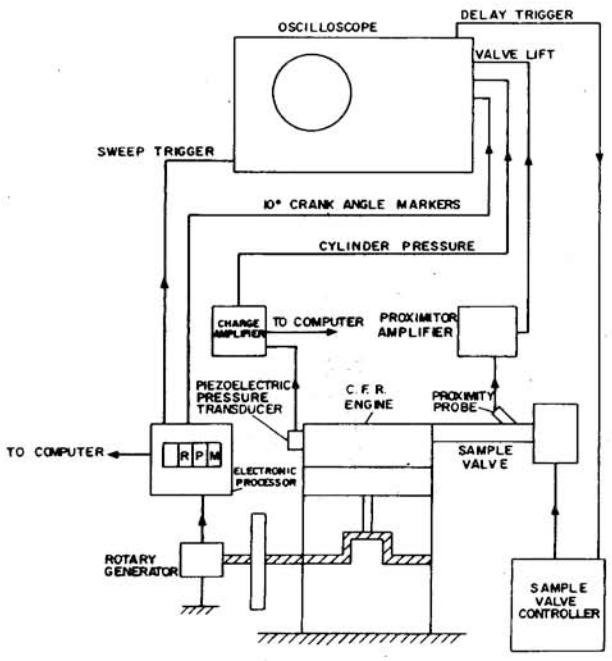

Fig. 4 - Block diagram of electronic and control systems

TYPICAL OSCILLOGRAM - Fig. 5 shows a typical oscillogram. Cylinder pressure, valve lift profile, crank angle markers, and spark timing were displayed. By observing the usual variations in the cylinder pressure trace, it is evident that the oscillogram shows four consecutive cycles. Note that variations in valve lift profile were negligible indicating reproducible sample valve operation. The valve closing time of .5 ms is consistent with the closing time calculated from the sample valve specifications. Oscillations in the valve lift profile after closing were due to bending of the needle shaft.

MASS AND VOLUME SAMPLED - The mass sampled per cycle, Δm_s, is given by the relationship

$$\Delta m_s = \rho_{sa} \Delta V_a = \rho_{sa} \dot{V}_d (2/\omega) \qquad (1)$$

where ρ_{sa} is the sample density at ambient conditions, ΔV_a is the volume sampled per cycle at ambient conditions, $\dot{V}_d$ is the sample flow rate measured by the displacement meter and ω is the engine speed. It should be noted that the flow through the ionization gauge was negligible and has been omitted in this calculation.

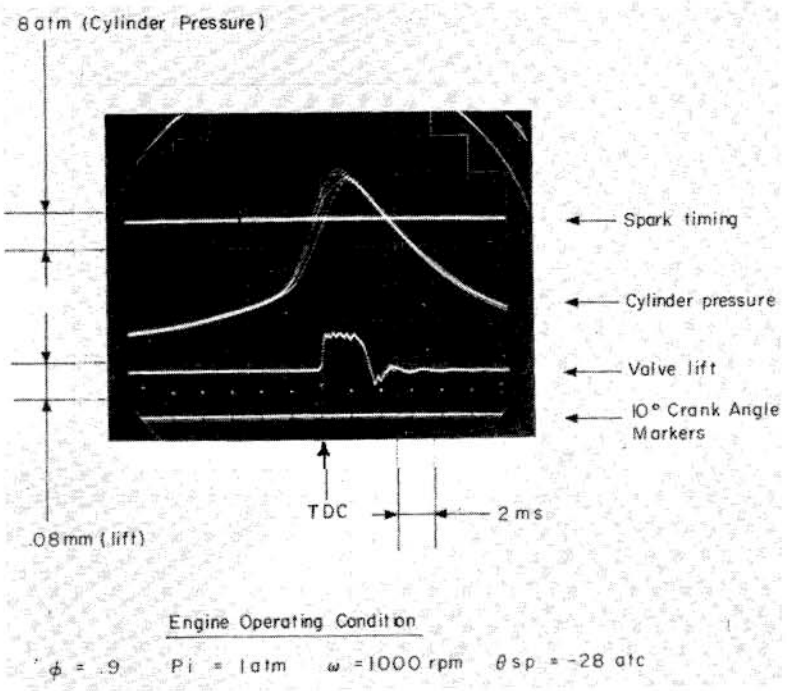

Fig. 5 - Typical oscillograph record

Fig. 6 shows a plot of Δm_s as a function of crank angle, θ, for a few operating conditions. Although the sampling valve parameters were not fixed, the dominating effect of cylinder pressure on Δm_s is seen.

The in-cylinder volume occupied by the sampled mass was computed using the equation

$$\Delta V_c = \Delta m_s / \rho_{sc} = \Delta V_a \rho_{sa} / \rho_{sc} \qquad (2)$$

where ρ_{sc} is the in-cylinder density when the sample was taken. During compression or expansion, ρ_{sc} was determined by mass conservation of the cylinder contents using the equation

$$\rho_{sc} = \rho_i \, (V_i / V_s) \qquad (3)$$

where ρ_i is the gas density at inlet valve close, V_i is the cylinder volume at inlet valve close, and V_s is the cylinder volume when sampling. For samples taken during blowdown and exhaust, isentropic expansion with an effective burned gas specific heat ratio $\gamma_b = 1.28$ was assumed.

Because the flow through the valve was choked under most sampling conditions, the in-cylinder sample volume ΔV_c ~50 mm^3 was very nearly constant throughout the entire engine cycle for fixed sample valve parameters.

As a first approximation, the flow into the sample valve was assumed to be radial and inviscid. Under these conditions, the

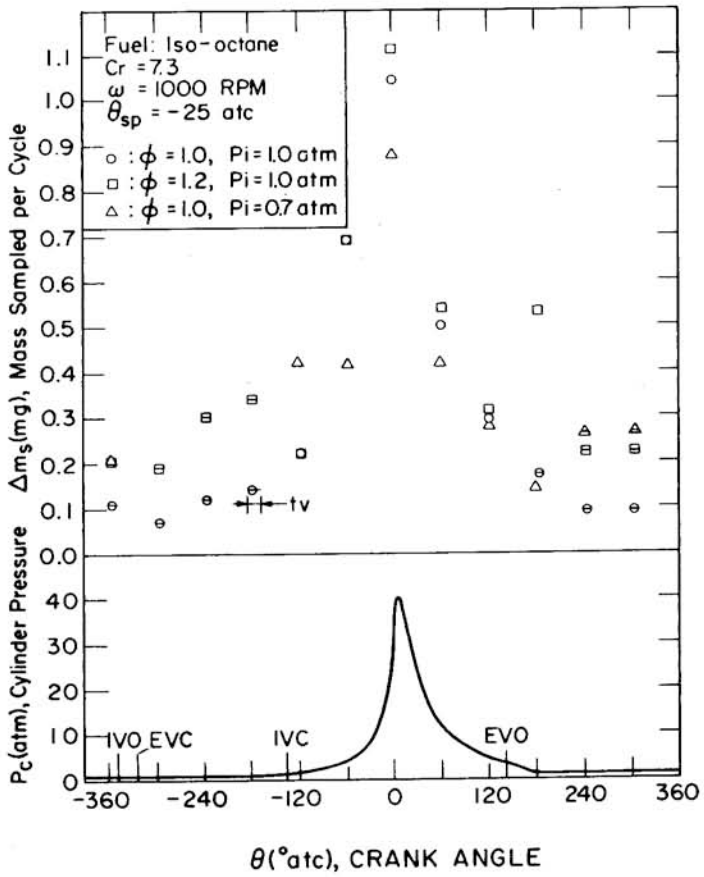

Fig. 6 - Typical data showing mass sampled per cycle as a function of crank angle

in-cylinder gas sample will occupy a hemispherical region of radius

$$r_c = (3\,\Delta V_c/2\pi)^{1/3} \qquad (4)$$

concentric with the valve orifice. For all the data presented, r_c was in the range 5-6 mm.

SAMPLE HYDROCARBON MOLE FRACTIONS - Some typical measurements of sample hydrocarbon mole fraction, f_{HCs}, are shown in Fig. 7. The bar through each measured value indicates the sample duration. Total hydrocarbon was measured in mole fractions of carbon atoms. Fluctuations in hydrocarbon mole fraction readings limited the accuracy to $\pm$ 10%. Hydrocarbon mole fractions were observed to rise from early intake values of 10^4 parts per million of carbon (ppmc) to approximately 10^5 ppmc during compression. The smooth increase suggests that the incoming charge was rapidly mixing with the residuals. Sample hydrocarbon was constant during compression indicating that mixing had been completed. The measured values agree well with those calculated for 15% residual gas. After the flame arrived at the sampling location, measured sample hydrocarbon mole fractions dropped to less than 10^3 ppmc. Expansion was characterized by increasing sample hydrocarbon mole fractions.

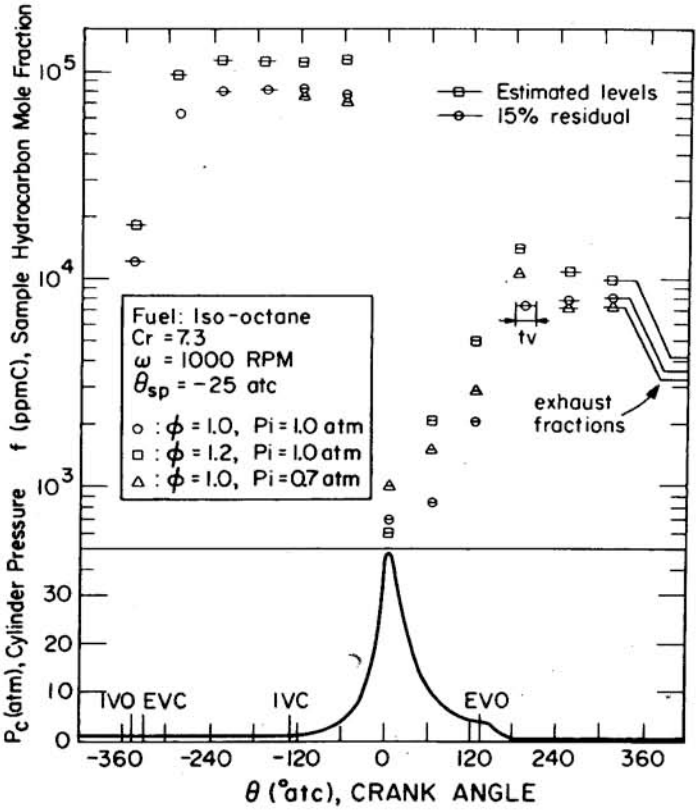

Fig. 7 - Hydrocarbon mole fractions in the sample gas as a function of crank angle for runs in Fig. 6. Also shown are average exhaust hydrocarbon mole fractions for these runs

This increase could be due either to an expanding quench layer on the cylinder wall or the discharge of unburned gas from crevice volumes as the pressure drops during the expansion stroke. As will be seen later, the results strongly suggest that the latter explanation is correct under the conditions of the present experiment.

Hydrocarbon concentrations immediately after exhaust valve opening were consistently higher than those measured later in the exhaust stroke. This is probably due to a puff of unburned gas discharged drom the sample valve thread crevice volume during cylinder blowdown. This puff would subsequently mix with the combustion products to produce the relatively constant levels observed later. Although not apparent in the data shown, hydrocarbon mole fractions at 300° ATC were generally about 10% higher than those at 240° ATC giving some evidence for the arrival of a hydrocarbon-rich wall-vortex at the sample valve location late in the cycle. The effect was much smaller than anticipated, however, probably due to in-cylinder oxidation of a large fraction of the unburned gas discharged from the piston ring crevice volume early in the expansion stroke. It may also be noted at this point that the hydrocarbon mole fractions at 120° ATC just prior to exhaust valve opening were approximately 25% of those measured during the latter part of the exhaust stroke. This fact will enter into the discussion later.

Fig. 7 also gives the average hydrocarbon concentrations measured in the exhaust products for the sample runs shown. It can be seen that they are approximately a factor 2 lower than the in-cylinder values at the end of the exhaust stroke.

CORRECTION FOR VALVE LEAKAGE - Because of the high mole fraction of hydrocarbon in the unburned charge, f_{HCu}, prior to arrival of the flame at the valve orifice, it was necessary that the valve have a very small leak rate to avoid large corrections to the measurements. In runs made with the valve closed, it was observed that the leak rate was proportional to the cylinder pressure, P_c. It was therefore assumed that the fraction of the hydrocarbon in the sample due to leakage, $f_{HC\ell}$, could be calculated from the equation

$$f_{HC\ell} \approx \varepsilon\, f_{HCu}\, \Delta m_\ell / f_{HCs}\, \Delta m_s \qquad (5)$$

where Δm_ℓ is the mass leaked per cycle, ε is the fraction of the mass leaked in an unburned condition and we have neglected the small difference in the molecular weights of various gas mixtures involved. The fraction ε was estimated

by numerical integration of the pressure data using the expression

$$\varepsilon = \int_{\theta_{IVO}}^{\theta_{FAV}} (P_c - P_{s\ell})\, d\theta \Big/ \oint (P_c - P_{s\ell})\, d\theta \quad (6)$$

where θ_{IVO} and θ_{FAV} are angles for inlet valve opening and flame arrival at the valve and P_s is the pressure in the sample line. The value of was approximately 0.3 for all engine conditions.

For the leaked hydrocarbon fraction to be less than 10%, Equation (5) requires

$$\Delta m_\ell / \Delta m_s < 0.3\ f_{HCS}/f_{HCu} \quad (7)$$

Originally, the sample valve had a stainless steel needle and a titanium alloy seat and condition (7) was very difficult to meet for typical values of f_{HCs}/f_{HCu} after flame arrival. Replacing the titanium seat with copper reduced the leakage to negligible values for all operating conditions reported.

SUMMARY OF MEASUREMENTS - The engine operating conditions investigated are summarized in Table 2 and the corresponding measured hydrocarbon mole fractions are shown in Fig. 7. All runs were made at an engine speed of 1000 RPM using isooctane as the fuel. The first five columns of Table 2 give the fuel/air equivalence ratio, ϕ, inlet pressure, P_i, spark angle after top center, θ_s, recirculated exhaust mole fraction, EGR, and estimated inlet gas temperature, T_i. The sixth and seventh columns give the measured mean-effective-pressure, IMEP, and the pressure at exhaust value opening, P_x. The eighth column gives the cylinder temperature at exhaust valve opening, T_x, calculated from the ideal gas equation of state

$$T_x = T_i\ (W_b/W_u)\ P_x\ V_x/P_i\ V_i \quad (8)$$

where W_b and W_u are the molecular weights of burned and unburned gas and P_x and V_x are the cylinder pressure and volume at exhaust valve opening. Finally, the ninth column gives the cylinder temperature after blowdown calculated from the equation

$$T_f = T_x\ (P_o/P_x)^{(\gamma_b - 1)/\gamma_b} \quad (9)$$

for isentropic expansion of the burned gas to atmospheric pressure P_o.

The in-cylinder and exhaust hydrocarbon mole fractions, $\bar{f}_{IC}$ and $\bar{f}_{EX}$, in parts per thousand carbon are shown in the lower part of Fig. 8 as a function of ϕ, P_i, θ_s, EGR, and T_i. $\bar{f}_{IC}$ is the average of the hydrocarbon mole fractions at 240 and 300° ATC and $\bar{f}_{EX}$ is the average hydrocarbon mole fraction in the exhaust stream. The values of the ratio $\bar{f}_{EX}/\bar{f}_{IC}$ are shown in the upper part of Fig. 8. The solid symbol denotes the common reference condition. The curves will be discussed in the next section.

Table 2 - Experimental Test Matrix

Fixed Parameters: Fuel = iso-octane
CR = 7.3
w = 1000 RPM

Parameter Varied		ϕ	P_i atm	θ_s °ATC	EGR %	T_i °K	IMEP atm	P_x atm	T_x °K	T_f °K
ϕ		0.8	1.00	-25	0	375	95	3.35	1200	921
		1.0	1.00	-25	0	375	103	3.60	1270	960
		1.2	1.00	-25	0	375	103	3.60	1270	960
P_i		1.0	0.50	-12	0	375	50	1.70	1200	1050
	*	1.0	0.72	-11	0	375	72	2.50	1230	1010
		1.0	1.00	-15	0	375	105	3.80	1350	1010
ϕ_s		1.0	0.72	-5	0	375	70	2.45	1200	990
	*	1.0	0.72	-11	0	375	72	2.50	1230	1010
		1.0	0.72	-25	0	375	72	2.50	1230	1010
EGR		1.0	0.72	-11	0	375	72	2.50	1230	1010
	*	1.0	0.78	-16	6	375	67	2.35	1130	937
		1.0	0.78	-16	11	375	63	2.20	973	890
T_i		1.0	0.72	-11	0	350	76	2.63	1210	976
	*	1.0	0.72	-11	0	375	72	2.50	1230	1010
		1.0	0.72	-11	0	405	68	2.37	1260	1040

*Reference Condition

ANALYSIS AND DISCUSSION

QUENCH LAYER ENTRAINMENT MODEL - In a preliminary analysis of these measurements [26], it was assumed that wall quench layers were the major source of hydrocarbon in the sampled gas. It was also assumed as a first approximation, that the flow into the sample valve was radial and invisid and that the sampled gas came from a hemispherical region concentric with the valve orifice. Under these conditions, the hydrocarbon mass per unit wall area is given by the equation

$$m_{HCs}/\pi r_c^2 = \frac{2}{3} f_{HCs}\ (W_C/W_b)\rho_{sc} r_c \quad (10)$$

where W_C is the molecular weight of carbon and ρ_{sc} and r_c are given by Equations 3 and 4. The characteristic quench layer thickness, δ_q, can be estimated from the relation

$$\delta_q \simeq m_{HCs}/\pi r_c^2\ \rho_{HC}(0) \quad (11)$$

where

$$\rho_{HC}(0) = f_{HCu}\ W_C\ P_c/RT_W \quad (12)$$

is the carbon density in the unburned gas at the wall, f_{HCu} is the mole fraction of carbon in the unburned gas, T_w is the wall temperature and R is the universal gas constant.

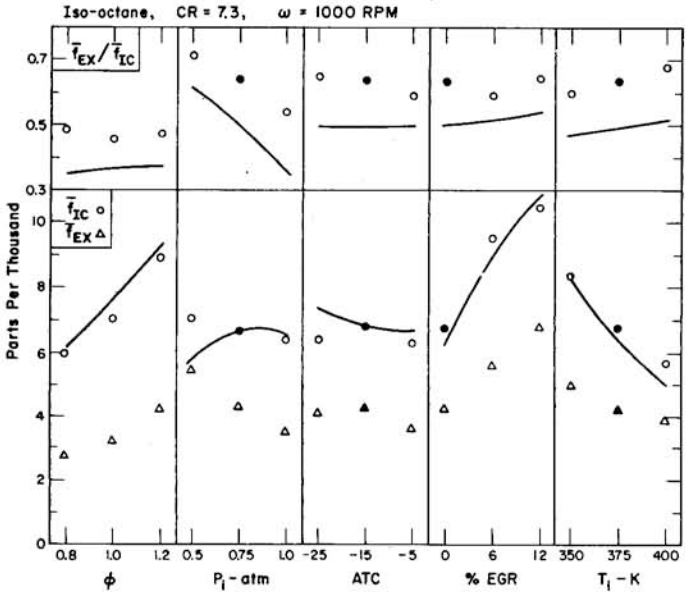

Fig. 8 - Lower part: Measured average in-cylinder and exhaust hydrocarbon mole fractions, $\bar{f}_{IC}$ and $\bar{f}_{EX}$, as a function of engine parameters for conditions shown in Table 2. Upper part: ratio of $\bar{f}_{EX}$ and f_{IC}. The reference condition is shown by the solid points. Curves show predictions of crevice hydrocarbon model

For Equation 10 to be valid, the quench layer thickness, δ_q, must be large compared to the characteristic thickness of the viscous boundary layer

$$\delta_v = \sqrt{\nu t_v} \tag{13}$$

where ν is the kinematic viscosity and t_v is the sampling time. Using Equations 11 and 13, the ratio

$$\beta \equiv \delta_q/\delta_v \tag{14}$$

was found to be of order 0.1. This showed that the effects of viscous drag on the quench layer at the wall could not be neglected. A viscous model of quench layer entrainment by flow into a point sink was therefore developed [27].

The details of the viscous flow model are given in the Appendix and the results are summarized graphically in Figure 9 for uniform, exponential and Gaussian quench layer hydrocarbon profiles. The parameter β is defined by Equation 14.

The function

$$F(\beta) \equiv (m_{HCs}/\pi r_c^2)/\rho_{HC}(0)\delta_v \tag{15}$$

is the ratio of the hydrocarbon mass per unit area calculated using the inviscid approximation to the product of the wall density of hydrocarbon times the viscous boundary layer thickness and the function

$$G(\beta) \equiv (m_{HC}/A)/(m_{HCs}/\pi r_c^2) \tag{16}$$

is the ratio of the corrected hydrocarbon mass per unit area to the corresponding inviscid value.

To make the correction, the value of $F(\beta)$ is first calculated from measured quantities. The corresponding value of β and $G^{-1}(\beta)$ can then be read directly from Fig. 9.

The values of β found in this way for a Gaussian profile ranged from 0.3 at 60° ATC to 1.0 for the exhaust stroke. The hydrocarbon mass per unit wall area was approximately $0.5\,\mu gC/cm^2$ for all crank angles and engine operating conditions.

If the quench layer interpretation were correct, Fig. 7 shows that the side wall quench layer was not exhausted from the cylinder since the hydrocarbon mole fractions in the sample gas were nearly constant during the exhaust stroke. Thus, the major contribution to exhaust hydrocarbon must have come from the headwall and the average mole fraction of hydrocarbon in the exhaust can be estimated from the expression

$$\bar{f}_{EXq} = (m_{HC}/A)\, A_h/P_i V_i\, (1 - r_f) \tag{17}$$

where A_h is the cylinder head area and r_f is the residual fraction of gas in the cylinder at the

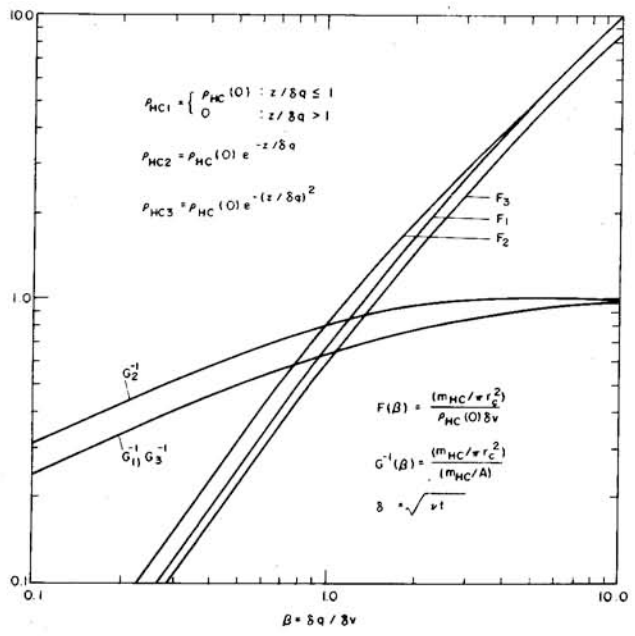

Fig. 9 - Functions for calculating quench layer entrainment by viscous flow into a point sink for (1) uniform, (2) exponential, and (3) Gaussian hydrocarbon profiles

end of the exhaust stroke. The values of $\bar{f}_{EXq}$ obtained from Equation 19 using the values of m_{HC}/A given by Equation 16 were of the order of 300 ppmC. This is less than 10% of the measured values of $\bar{f}_{EX}$ shown in Fig. 8 and indicates that quench layers could not have been the major source of the exhaust hydrocarbon observed.

This conclusion is supported by a comparison of the in-cylinder sample hydrocarbon mole fractions measured in the present experiments with the corresponding values measured by LoRusso et al. [22] using a faster sampling value but a similar CFR engine. In the experiments of LoRusso et al., the mass sampled during the exhaust stroke was less than 10% of the mass sampled in the present experiments. Thus, if quench layers were the source of the hydrocarbon observed, the hydrocarbon mole fractions measured by LoRusso et al. should have been substantially larger than the values of $\bar{f}_{IC}$ shown in Fig. 8. In fact, they were only one tenth as large.

Finally, theoretical calculations [21] indicate that, under engine-like conditions, the hydrocarbon left at a wall after flame quenching will be almost completely oxidized due to diffusion into the hot combustion products. This has been confirmed by recent measurements in constant volume bombs [23-25] which give an upper bound for m_{HC}/A of the order of 0.02 μgC/cm . This is less than 5% of the value 0.5 μgC/cm deduced from the sample hydrocarbon mass using the viscous quench layer model presented.

HYDROCARBON FROM CREVICE VOLUMES - The analysis presented in the previous section strongly indicates that quench layers could not have been the major source of the hydrocarbon observed in these experiments. The most likely alternative is that unburned gas in fine crevices into which a flame cannot propagate were the source and a model for estimating in-cylinder and exhaust hydrocarbon levels resulting from the discharge of such crevices has been developed.

The basic assumption of the model is that exhaust hydrocarbon mole fractions are controlled primarily by in-cylinder oxidation rates. Oxidation times, τ_R, for typical fuel hydrocarbons have been measured under engine-like conditions and may be correlated by an equation of the form [28, 29]

$$\tau_R^{-1} = \frac{1}{[HC]} \frac{d[HC]}{dt} = A(P_{O_2}/P_o)^b \, e^{-E/RT} \quad (18)$$

where P_{O_2} is the partial pressure of oxygen. Unfortunately, there is a great deal of scatter in the results and the parameters A, b, and E are not well determined. However, a reasonable set of values which represents the data in the neighborhood of 1200 K is $A = 2 \times 10^8$ sec^{-1}, b = 0.25, and E = 32,000 cal/g mole.

Prior to blowdown, in-cylinder temperatures will generally exceed 1250 K and Equation 18 predicts that τ_R will be less than a millisecond. Thus, any hydrocarbons entering the cylinder during the expansion stroke from crevices will be strongly oxidized leading to relatively low levels of in-cylinder hydrocarbon at the time the exhaust valve opens. During blowdown, the temperature falls rapidly to values typically less than 1000 K and Equation 18 predicts values of τ_R greater than 50 milliseconds. Under these conditions, a large fraction of the hydrocarbon discharged from crevices into the cylinder during blowdown can be expected to survive with little further oxidation during the exhaust stroke. This prediction is supported by the data shown in Fig. 7.

On the basis of the above model, it is possible to estimate the mole fraction of in-cylinder hydrocarbon, $\bar{f}_{IC}$. We assume that turbulent mixing is sufficiently rapid to produce a reasonably uniform composition throughout the cylinder in a time somewhat less than $(2\omega)^{-1}$ and that "sudden freezing" of oxidation reactions occurs when the temperature drops below the sudden freezing temperature, T_{SF}. At this time, the number of moles of hydrocarbon in the cylinder will be zero and the number of moles of gas in the crevices will be

$$N_{CR} = P_{SF} \, V_{CR}/RT_W \quad (19)$$

where P_{SF} is the cylinder pressure at T_{SF} and V_{CR} is the crevice volume. If P_{SF} is less than the pressure at ignition, as is the case in practice, then the gas in the crevices will be pure unburned charge. Assuming the gas in the crevices expands isothermally to atmospheric pressure during blowdown, the number of moles of hydrocarbon discharged into the cylinder after freezing has occurred will be

$$N_{CIC} = f_{HCu} \, N_{CR} \, (1 - P_o/P_{SF}) \quad (20)$$

where f_{HCu} is the mole fraction of carbon in the unburned charge. The number of moles of gas in the cylinder after blowdown will be

$$N_f = N_x \, (P_o/P_x)^{1/\gamma_b} \quad (21)$$

where

$$N_x = (W_u/W_b) \, P_i V_i/RT_i \quad (22)$$

is the number of moles of burned gas in the cylinder prior to blowdown. Dividing Equation 20 by 21, we obtain

$$\bar{f}_{IC} = \frac{N_{CIC}}{N_f} = f_{HCu} \left(\frac{N_{CR}}{N_X}\right)\left(\frac{P_x}{P_o}\right)^{1/\gamma_b} \left(1 - \frac{P_o}{P_{SF}}\right) \quad (23)$$

Finally, using Equations 19 and 22 and the relations.

$$P_{SF}/P_o = (T_{SF}/T_f)^{\gamma_b/(\gamma_b-1)} \quad (24)$$

and

$$P_x/P_i = W_u T_x/W_b T_i \quad (25)$$

we find

$$\bar{f}_{IC} = f_{HCu} \frac{V_{CR} T_x}{V_i T_w} \left(\frac{W_b P_o T_i}{W_u P_i T_x} \right)^{\frac{\gamma_b - 1}{\gamma_b}} \left(\left(\frac{T_{SF}}{T_x} \right)^{\frac{\gamma_b}{\gamma_b - 1}} - 1 \right) \quad (26)$$

The sudden freezing temperature can be estimated by equating the characteristic reaction time, τ_R, to the blowdown time for the cylinder, τ_B. Using Equation 18 and setting $\tau_R = \tau_B \sim 3$ msec., we obtain

$$T_{SF} = 1320/(1 + .02 \ln (f_{O_2} P_i/100P_o)) \quad (27)$$

where T_{SF} is in °K and f_{O_2} is the mole fraction of O_2 in percent. The measured values of f_{O_2} in the exhaust for equivalence ratios ϕ = 0.8, 1.0, and 1.2 were f_{O_2} = 6.0, 1.2, and 0.2 percent respectively.

Substituting Equation 28 into Equation 27 and using the data in Table 2, we obtain the results shown by the solid curves in the lower part of Fig. 8. A crevice volume of 6 cm^3 was used to fit the data.

Considering the simplicity of the model and the uncertainty in the value of τ_R, Equation 17 reproduces the trends in the data remarkably well. The dominating effects are those of exhaust temperature and equivalence ratio which determine the sudden freezing point. The implied crevice volume is quite high but not excessively so for a well worn test engine with six threaded ports. The estimated volume of the piston ring crevice was 0.74 cm^3. In addition, there were two 18 mm spark plug ports having an estimated thread crevice volume of 0.25 cm^3 per port and four 25 mm access ports having an estimated thread crevice volume of 0.5 cm^3 per port. This gives a total crevice volume V_{CR} = 3.25 cm^3 which is about half the value required to fit the measurements. Again considering the uncertainties involved in the measurements and the estimates of the crevice volumes, this is not unreasonable.

We can also use this model to calculate the ratio of exhaust to in-cylinder hydrocarbon. We assume that the in-cylinder hydrocarbon mole fraction prior to blowdown is small so that the number of moles of hydrocarbon entering the exhaust system during blowdown is negligible and that the number of moles of hydrocarbon entering the exhaust system during the exhaust stroke is given by

$$N_{CE} = \bar{f}_{IC} N_f (1 - r_f) \quad (28)$$

Dividing N_{CE} by the number of moles of gas entering the exhaust system per complete engine cycle,

$$N_E = N_x (1 - r_f) \quad (29)$$

and using Equation 21, we obtain

$$\bar{f}_{EX} = N_{CE}/N_E = \bar{f}_{IC} (P_o/P_x)^{1/\gamma_b} \quad (30)$$

The ratio

$$\bar{f}_{EX}/\bar{f}_{IC} = (P_o/P_x)^{1/\gamma_b} \quad (31)$$

is shown by the solid lines in the upper part of Fig. 8. It can be seen that the dependence of the data on engine parameters is predicted reasonably well but that the measured values are about 25% higher than the predicted values. This is consistent with the data in Fig. 7 which shows that the in-cylinder hydrocarbon mole fractions observed at 120° ATC just prior to exhaust valve opening are about 25% of those measured later in the exhaust stroke. This additional hydrocarbon is probably due to incomplete oxidation of crevice hydrocarbon discharged late in the expansion stroke.

It is of considerable interest to note that the values of $\bar{f}_{EX}/\bar{f}_{IC}$ observed in these experiments are almost identical to the value $\bar{f}_{EX}/\bar{f}_{IC} \sim 0.6$ obtained by LoRusso et al. [22] in a similar CFR engine operating at 1250 RPM on propane at equivalence ratios of 0.90 and 1.28. However, due presumably to a very much smaller crevice volume, the absolute hydrocarbon levels measured by LoRusso et al. were only one tenth the levels measured in the present experiment. This agrees with the predictions of the simple crevice volume model proposed, but is completely inconsistent with the predictions of the quench layer model.

CONCLUSIONS

It is highly probable that crevice volumes were the major source of both the in-cylinder and exhaust hydrocarbon observed in these experiments. The upper bound determined for the quench layer contribution was 0.5 $\mu gC/cm^2$ which is roughly 20 times that expected on the basis of recent experiments in bombs [25] and engines [22]. The main general conclusions which can be drawn, apart from the obvious

one that experiments of this kind should be conducted in engines with fewer crevices, are:

1) Mixing processes in engine cylinders are quite rapid, producing reasonably uniform composition within a crank angle of ~60°.

2) Prevailing temperatures within the cylinder prior to blowdown are sufficiently high to cause virtually complete oxidation of any hydrocarbon either from crevices or quench layers which mix with the burned gas. As a consequence, the burned gases exhausted during blowdown and early in the exhaust stroke have relatively low hydrocarbon mole fractions.

3) In present engines, the major contribution to both in-cylinder and exhaust hydrocarbon comes from unburned gas discharged from crevices into the cylinder during the expansion stroke after the cylinder temperature has dropped sufficiently to freeze oxidation reactions.

4) A relatively simple "sudden freezing" model of crevice hydrocarbon based on the above observations accounts reasonably well for the magnitude and trends of both in-cylinder and exhaust hydrocarbon mole fractions.

5) The observed ratio of exhaust to in-cylinder hydrocarbon mole fractions indicates a small contribution to exhaust hydrocarbon during the blowdown process. This could be due to the discharge of crevices in close proximity to the exhaust valve.

6) Substantial reduction of exhaust hydrocarbon from practical engines should be possible by elimination or reduction of crevices such as those associated with spark plug threads, piston ring, valve seat, and head gasket.

ACKNOWLEDGEMENT

This work was supported by a grant from the General Motors Research Laboratory which also designed and built the sample valve used.

REFERENCES

[1] W. A. Daniel, Sixth Symposium (International) on Combustion, Reinhold Publishing Corp., 1957.

[2] W. A. Daniel and J. T. Wentworth, SAE Technical Progress Series, Vol. 6, "Vehicle Emissions," New York, 1964.

[3] W. A. Daniel and J. T. Wentworth, SAE Transactions, Vol. 63, 1964.

[4] J. T. Wentworth, SAE Transaction 77, Paper 68109, 1968.

[5] J. T. Wentworth, Combustion Science and Technology 4, 97, 1970.

[6] E. W. Kaiser, A. A. Adamczyk, and G. A. Lavoie, 18th Symposium (International) on Combustion, Waterloo, Canada, August 1980.

[7] O. I. Smith, C. K. Westbrook, and F. R. Sawyer, The Combustion Institute, Canadian Section, Banff, Canada, May 1977.

[8] R. Freidman and W. C. Johnston, "The Wall Quenching of Laminar Propane Flames as a Function of Pressure, Temperature, and Air-Fuel Ratio," Journal of Applied Physics, 21, 1950.

[9] R. Freidman and W. C. Johnston, "Pressure Dependence of Quenching Distance of Normal Heptane, Iso-octane, Benzene, Ethyl Ether Flames," Journal of Chemistry and Physics, 20, 919, 1952.

[10] K. A. Green and J. T. Agnew, "Quenching Distance of Propane-Air Flames in a Constant Volume Bomb," Combustion and Flame, 15, 189, 1970.

[11] A. D. Goolsby and W. A. Haskell, "Flame-Quenching Distance Measurements in a CFR Engine," Combustion and Flame, 26, 1976.

[12] A. E. Potter, Jr. and A. L. Berlad, A.C.A. TN 3398, 1955.

[13] A. P. Kurkov and W. Mursky, 12th Symposium (International) on Combustion, 1968.

[14] C. R. Ferguson and J. C. Keck, Combustion and Flame, 28, 197, 1977.

[15] C. R. Ferguson and J. C. Keck, Combustion and Flame, 34, 85, 1979.

[16] J. T. Agnew, SAE, Paper 670125, 1967.

[17] W. A. Daniel, SAE Paper 700108, 1970.

[18] R. J. Tabaczynski, J. B. Heywood, and J. C. Keck, SAE Transactions, Paper 750009, 1975.

[19] J. B. Heywood, Progressive Energy Combustion Science, Vol. 1, 1976.

[20] A. A. Adamczyk, and G. A. Lavoie, SAE Transactions 87, Paper 780969, 1978.

[21] C. K. Westbrook, A. A. Adamczyk, and G. A. Lavoie, The Combustion Institute, Western Section, Berkeley, October 1979.

[22] J. A. LoRusso, E. W. Kaiser, and G. A. Lavoie, The Combustion Institute, Eastern Section, Atlanta, November 1979. Also Paper 800045, SAE Congress, Detroit, February 1980.

[23] P. Bergner, H. Eberino, and H. Pokorny, Third Alcohols Symposium, Asilomar, May 1979.

[24] A. A. Adamczyk, E. W. Kaiser, J. A. Cavolowsky, and G. A. Lavoie, 18th Symposium (International) on Combustion, Waterloo, Canada, August 1980.

[25] M. Sellnau, G. Springer, and J. C. Keck, SAE Congress, Detroit, February 1981.

[26] A. K. Wrobel, P. Weiss, and J. C. Keck, The Combustion Institute, Central State Section, April 1979.

[27] P. Weiss, M.S. Thesis, Department of Mechanical Engineering, Massachsuetts Institute of Technology, Cambridge, Massachusetts, January 1980.

[28] G. A. Lavoie, Paper 780229, SAE Congress, Detroit, February 1978.

[29] R. J. Herrin, D. J. Patterson, and R. H. Kadlec, "Combustion Modeling in Reciprocating Engines," Plenum Press, New York, 1980.

APPENDIX

BOUNDARY LAYER ANALYSIS FOR FLOW INTO A POINT SINK

A similarity solution of the boundary layer equations for two-dimensional incompressible flow into a point sink on a plane surface results in the following expressions for the velocities u and w parallel and perpendicular to the wall [A1].

$$u = -(a/x^2)\ f'(\eta) \tag{A1}$$

$$w = -(a\nu/x^3)^{\frac{1}{2}}\ (f(\eta) - 3\ f'(\eta)) \tag{A2}$$

when $f(\eta)$ is the solution of the equation

$$f''' - ff'' + 4(1-(f')^2) = 0 \tag{A3}$$

which satisfies the boundary conditions: $f(0) = f'(0) = 0$ and $f'(\infty) = 1$,

$$\eta = z\ (a/2\nu\ x^3)^{\frac{1}{2}} \tag{A4}$$

is the similarity variable, x and z are the coordinates parallel and perpendicular to the wall, a is the sink strength, and ν is the kinematic viscosity.

For $r = (x^2 + z^2)^{\frac{1}{2}} << a/2\nu$, the boundary layer will be thin and the radial velocity at any point in the flow can be approximated by the equation

$$\dot{r} \simeq -af'(\eta)/r^2 \tag{A5}$$

In this case, the total mass flow rate into the sink is given by

$$\dot{m}_s = -2 \int_0^{\pi/2} \rho_{sc} \dot{r}\ r^2\ \sin\phi d\phi \simeq 2\pi\rho_{sc} a \tag{A6}$$

and the sink strength, a, is given approximately by

$$a \simeq \dot{m}_s/2\pi\rho_{sc} \tag{A7}$$

For a constant sink strength, the mass entering the sink in a time interval t_v is

$$\Delta m_s \simeq 2\pi\ a\ \rho_{sc}\ t_v \tag{A8}$$

and the radius of a hemispherical volume occupied by this mass is

$$r_c \simeq (3\Delta m_s/2\pi\rho_{sc})^{1/3} = (3at_v)^{1/3} \tag{A9}$$

To determine the hydrocarbon mass flow rate into a sink on a surface where there is a thin quench layer, the initial locus of the last fluid particles to enter the sink must be found. This may be done by integrating Equation A5 along a streamline [A2]. To a first approximation, $f'(\eta)$ may be assumed constant along a streamline and we obtain using Equation A9

$$r^3 \simeq 3\ a\ t_v f'(\eta) = r_c^{\ 3}\ f'(\eta) \tag{A10}$$

Numerical results for $f'(\eta)$ are given in reference [A1] and can be very accurately represented by

$$f'(\eta) = 1 - \exp(-\sqrt{6}\ \eta). \tag{A11}$$

In the boundary layer, $x \simeq r$ and Equations A4, A10, and A11 can be combined to give

$$z \simeq -\delta_v \left(\frac{r}{r_c}\right)^{3/2} \ell n\left(1 - \left(\frac{r}{r_c}\right)^3\right) \tag{A12}$$

where

$$\delta_v = (\nu\ t_v)^{\frac{1}{2}} \tag{A13}$$

is the characteristic thickness of the velocity boundary layer at time t_v. Note that Equation A12 implies

$$z/\delta_v \simeq (r/r_c)^{9/2} : z/\delta_v < 1$$

and

$$r \simeq r_c : z/\delta_v > 1$$

A plot of Equation A12 is shown in Fig. A1.

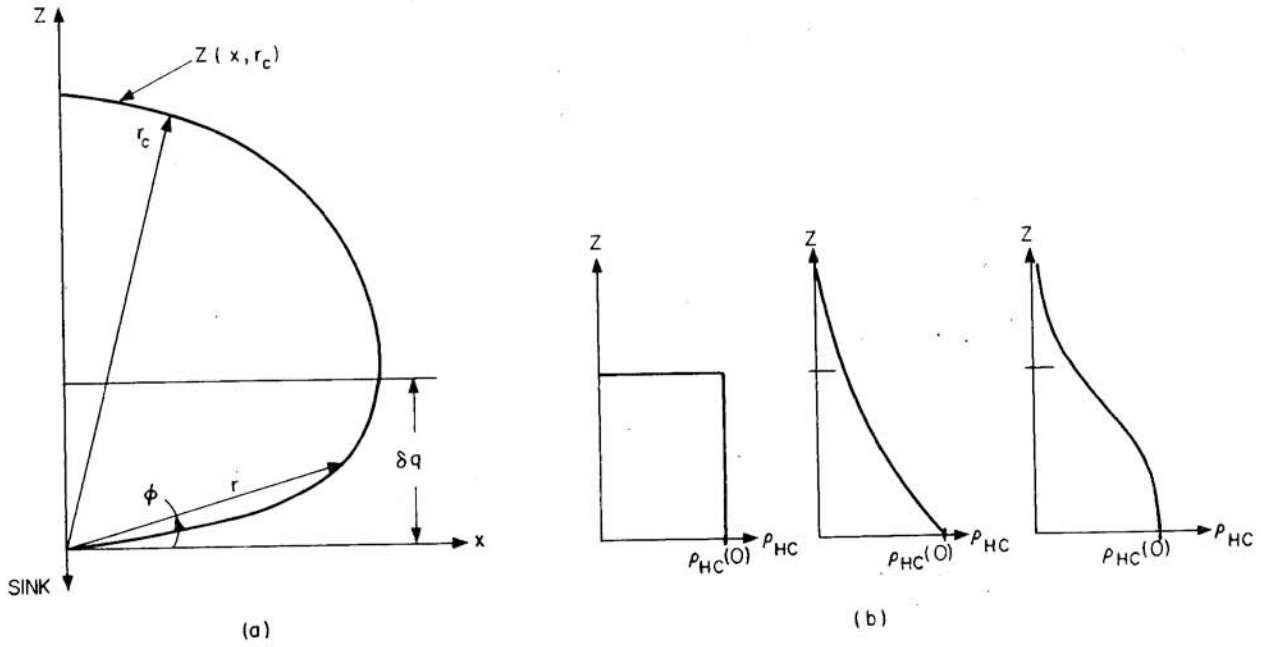

Fig. A1 - Schematic diagrams showing: (a) original loci of last fluid elements to enter the sink and (b) assumed hydrocarbon profiles

The mass of hydrocarbon entering the sink can now be calculated by integrating the initial hydrocarbon density, $\rho_{HC}(z)$, over the volume defined by Equation A12. This gives

$$m_{HC} = \int_0^{r_c} \int_0^{x(z)} \rho_{HC}(z)\, 2\pi\, x\, dx\, dz$$

$$= \pi r_c^2 \int_0^{r_c} \rho_{HC}(z)\, \tilde{x}^2\,(z)\, dz \qquad \text{(A14)}$$

where we have introduced the dimensionless coordinate

$$\tilde{x}(z) = x/r_c \qquad \text{(A15)}$$

Introducing a second dimensionless coordinate

$$\zeta = z/\delta_q \qquad \text{(A16)}$$

where δ_q is a characteristic quench layer thickness such that $\rho_{HC}(z) << \rho_{HC}(0)$ for $z > \delta_q$, and assuming $\delta_q << r_c$, Equation A14 becomes

$$\frac{m_{HC}}{\rho_{HC}(0)\pi r_c^2 \delta_v} = \beta \int_0^{\infty} \tilde{\rho}(\zeta)\, \tilde{x}^2\,(\beta\zeta)\, d\zeta \equiv F(\beta) \qquad \text{(A17)}$$

where

$$\beta = \delta_q/\delta_v \qquad \text{(A18)}$$

is the ratio of the quench layer thickness to the boundary layer thickness,

$$\tilde{\rho}(\zeta) = \rho_{HC}(\zeta\delta_q)/\rho_{HC}(0) \qquad \text{(A19)}$$

is the normalized hydrocarbon density and $\tilde{x}(\beta\zeta)$ is the solution of the equation

$$\beta\zeta = -\tilde{x}^{3/2}\, \ell n(1-\tilde{x}^3) \qquad \text{(A20)}$$

The mass of hydrocarbon per unit area is given by

$$\frac{m_{HC}}{A} = \int_0^{\infty} \rho_{HC}(z)\, dz = \rho_{HC}(0)\, \delta_q \int_0^{\infty} \tilde{\rho}(\zeta)\, d\zeta \qquad \text{(A21)}$$

Finally, combining Equations A17, A18, and A21 gives

$$\frac{m_{HC}/A}{m_{HC}/\pi r_c^2} = \frac{\beta}{F(\beta)} \int_0^{\infty} \tilde{\rho}(\zeta)\, d\zeta \equiv G(\beta) \qquad \text{(A22)}$$

The functions $F(\beta)$ and $G(\beta)$ have been numerically evaluated for three hydrocarbon density profiles,

$$\tilde{\rho}_1 = \begin{cases} 1 & : \quad \zeta \le 1 \\ 0 & : \quad \zeta > 1 \end{cases} \qquad \text{(A23)}$$

$$\tilde{\rho}_2 = \exp(-\zeta) \qquad \text{(A24)}$$

$$\tilde{\rho}_3 = \exp(-\zeta^2)$$

These profiles are shown schematically in Fig. A1. $F(\beta)$ and $G^{-1}(\beta)$ are plotted in Fig. 9 and asymptotic expressions valid for $\beta << 1$ and $\beta >> 1$ are given in Table A1.

REFERENCES

APPENDIX

[A1] L. Rosenhead, "Laminar Boundary Layers," Oxford University Press, 1963.

[A2] R. E. Hick, R. F. Probstein, and J. C. Keck, Paper 750009, SAE Congress, Detroit, February 1975.

Table A1 - Asymptotic Expressions for $F(\beta)$ and $G(\beta)$

$$F(\beta) \equiv \beta G^{-1}(\beta) \int_0^\infty \tilde{\rho}\, d\zeta$$

Profile	$\int_0^\infty \tilde{\rho}\, d\zeta$	$\beta << 1$: $G^{-1}\beta^{-4/9}$	$\beta >> 1$: G^{-1}
1 Uniform	1	.69	1
2 Exponential	1	.89	1
3 Gaussian	.89	.71	1

Society of Automotive Engineers, Inc.
400 COMMONWEALTH DRIVE, WARRENDALE, PA 15096

16 page booklet.

Printed in U.S.A.